Applied Mathematical Modelling 36 (2012) 2370–2383

Contents lists available at SciVerse ScienceDirect

Applied Mathematical Modelling

journal homepage: www.elsevier.com/locate/apm

Intelligent active force control of a 3-RRR parallel manipulator incorporating fuzzy resolved acceleration control

Amin Noshadi, Musa Mailah *, Ali Zolfagharian

Department of System Dynamics and Control, Faculty of Mechanical Engineering, Universiti Teknologi Malaysia (UTM), 81310 UTM Johor Bahru, Johor, Malaysia

ARTICLE INFO

Article history:
Received 22 December 2010
Received in revised form 10 August 2011
Accepted 16 August 2011
Available online 23 August 2011

Keywords:
Robust motion control
Resolved acceleration control
Fuzzy tuning
Active force control
3-RRR planar parallel manipulator

ABSTRACT

This paper introduces a novel intelligent control scheme for robust and precise positioning and orientation of a class of highly non-linear 3-RRR (revolute-revolute-revolute) planar parallel manipulator. The primary objective is to force the manipulator to track accurately a prescribed Cartesian trajectory when the system is subjected to different types of disturbances in the forms of forced harmonic excitations. A two level fuzzy tuning resolved acceleration control (FLRAC) is first designed and implemented to the system to demonstrate the stable response of the manipulator in performing trajectory tracking tasks in the absence of the disturbances. In this scheme, the first level of fuzzy tuning is used to acquire the proportional-derivative (PD) gains linearly while the second level considers non-linear tuning for determining the other parameters of the fuzzy controller to increase its performance. Then, the controller is added in series with an active force controller (AFC) to create a novel two degree-of-freedom (DOF) controller known as FLRAC-AFC which is subsequently and rigorously tested for system robustness and accuracy in tracking the prescribed trajectory. The simulation study provides further insight into the potentials of the proposed robotic system in rejecting the disturbances for the given operating conditions. The results clearly show that the FLRAC-AFC scheme provides a much superior trajectory tracking capability compared to the conventional linear RAC alone.

1. Introduction

Parallel manipulator is essentially a closed-loop kinematic chain mechanism in which the end-effector is linked to the base by several independent kinematic chains [1]. Due to the special characteristics of parallel manipulators such as high rigidity, high accuracy and great carrying payload capability, they have attracted significant attention and interest amongst the researchers in the past decade. After the published works on parallel mechanisms proposed by Gough and Stewart [2,3], various types of parallel manipulators have been designed and practically utilized in industrial applications such as assembly, packaging and machining operations. For instance, a 3-DOF parallel robot was designed to manipulate and hold the heavy work pieces as reported in [4]. Another 3-DOF planar parallel robot in micro size was built and developed for low-torque precision positioning tasks [5]. One of the most interesting advantages of parallel manipulators over the serial counterparts is the possibility to locate the actuators on the base, which is suitable for fast and accurate operations. However, the kinematics and dynamics of parallel manipulators are very complex due to their inherent closed-loop kinematic chains.

Control of parallel manipulators has only been addressed by few researchers in the literature. Nevertheless, Ghorbel showed that the common methods used for control of serial robots can be utilized to parallel robots as well [6]. Walker presented a robust independent joint control scheme to a high-speed parallel robot. He showed that the common

* Corresponding author. Tel.: +60 7 5534735; fax: +60 7 5566159.
E-mail addresses: namin7@live.utm.my (A. Noshadi), musa@fkm.utm.my (M. Mailah), ali.zolfagharyan@gmail.com (A. Zolfagharian).

0307-904X/$ - see front matter © 2011 Elsevier Inc. All rights reserved.
doi:10.1016/j.apm.2011.08.033

independent joint control method such as the proportional-integral-derivative (PID) controller is not able to achieve the desired and satisfactory performance because of their low capability to reject the environment uncertainties and disturbances [7]. Honegger et al. introduced an adaptive control method on a 6-DOF high speed milling parallel manipulator [8]. They focused on the advantage of the parallel robots over the serial counterparts which is the possibility of the former to keep the motors fixed to the base in order to perform fast movements by the use of lightweight links. Yoo et al. applied a fuzzy controller to a two-link planar robot manipulator to compensate for the unknown dynamic parameters of the system [9]. Stan et al. applied a fuzzy control method over traditional PID control to a 3-DOF isoglide medical parallel robot, and they obtained better results in the fuzzy-based controller compared to the classic PID controller [10].

In this paper, a robust motion control of a 3-RRR planar parallel manipulator is studied. In the first step, a linear RAC scheme was applied to the system to control the trajectory tracking of the end-effector in Cartesian space in an ideal situation, i.e., in the absence of disturbances. Then a two level fuzzy controller was developed to tune the PD outer-loop gains. For fuzzy approach, the normalizing parameters were determined according to the maximum position and orientation errors of the end-effector for the first level of tuning which called linear tuning. In the second level of tuning, other parameters of the fuzzy controller are determined and substituted to increase the performance of the fuzzy controller. Finally, in order to provide a robust controller in the presence of disturbances, the fuzzy logic tuned RAC (FLRAC) scheme was embedded in another novel control scheme called the active force control (AFC) to enhance the performance of the overall system for tracking a prescribed trajectory when the system is subjected to a number of disturbances. The robustness and effectiveness of the FLRAC-AFC strategy as a 'disturbance rejector' is presented through a simulation study using MATLAB/Simulink software package. The results clearly show that although the proposed FLRAC scheme is very useful in general operations, i.e., in the absence of disturbances, the system performance degrades considerably when the disturbances are applied to the manipulator. However, when the system is integrated with the AFC-based controller, the system performance significantly improves in spite of the adverse operating and loading conditions.

2. Modelling of 3-RRR planar parallel manipulator

2.1. Inverse kinematics

A three DOF planar parallel manipulator is depicted in Fig. 1. The system has nine revolute joints, i.e., three actuated joints fixed to the base and six unactuated joints that form three closed kinematic chains. The triangular plate, which is located in the middle of the figure is supposed to be the end-effector of the system. The manipulator is symmetric and also each leg of the manipulator has the same length.

The aim of solving the inverse kinematics is to obtain the angles of active joints from the position and orientation of the end-effector, which are essential for the position control of the parallel manipulators. The inverse and direct kinematic analyses of the manipulator have been derived and presented in [11].

Solving the inverse kinematics is very useful since the robot tasks are commonly formulated in terms of end-effector's specified position and motion.

2.2. Direct kinematics

Most of the parallel manipulators have easier inverse kinematic solutions compared to serial mechanisms, while the direct kinematic problems are very challenging in the majority of parallel robots. In direct kinematic problem, with given

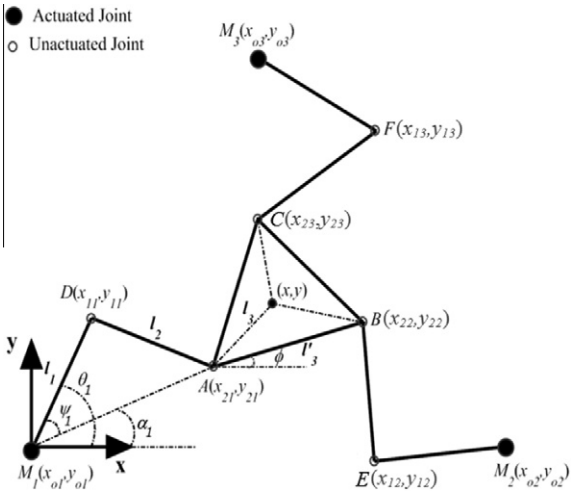

Fig. 1. General form of a planar three DOF parallel manipulator.

position of joint angles, the position and direction of the end-effector can be obtained without regarding the forces or masses. Unlike the serial manipulators, there is no unique solution for direct kinematics of the parallel robots. Although, several computational methods have been proposed to determine the pose of end-effector in Cartesian space, these methods are more often than not, very time consuming. For direct kinematics of a 3-RRR manipulator, Gosselin showed that a maximum of six results are possible [11]. However, due to the trajectory tracking procedure, only one of the solutions is deemed the correct solution. In this study, the previous position of the platform is used as the initial conditions which enable us to have a better chance to find the correct solution. From Fig. 1, if the three actuated joint angles are specified, the positions of points D, E and F can be easily computed. Furthermore, the chain D-A-B-E could be considered as a four-bar linkage as illustrated in Fig. 2.

2.3. Velocity inversion

To map the velocities in joint space into Cartesian space, the Jacobian matrix of the manipulator is used. The Jacobian matrix can be determined as follows:

$$J\dot{x} = \dot{\theta}, \tag{1}$$

where $\dot{x}$ is the vector of velocities in Cartesian space in which for a 3-RRR manipulator, it is defined by $\dot{x} = [\dot{x}, \dot{y}, \dot{\phi}]^T$ and $\dot{\theta}$ is the vector of joint velocities, $\dot{\theta} = [\dot{\theta}_1, \dot{\theta}_2, \dot{\theta}_3]^T$.

By differentiation of the equations of the coordinates with respect to time, the Jacobian matrix can be obtained [11].

$$J = \begin{bmatrix} r_1/u_1 & s_1/u_1 & t_1/u_1 \\ r_2/u_2 & s_2/u_2 & t_2/u_2 \\ r_3/u_3 & s_3/u_3 & t_3/u_3 \end{bmatrix}, \tag{2}$$

where

$$r_i = x - x_{oi} - l_1 cos\ \theta_i - l_3 cos\ \phi_i, \tag{3}$$
$$s_i = y - y_{oi} - l_1 sin\ \theta_i - l_3 sin\ \phi_i, \tag{4}$$
$$t_i = -l_3\ [(y - y_{oi}) cos\ \theta_i - (x - x_{oi}) sin\ \phi_i] + l_1 l_3 \sin\ (\theta_i - \phi_i), \tag{5}$$
$$u_i = -l_1 [(y - y_{oi}) cos\ \theta_i - (x - x_{oi}) sin\ \theta_i] + l_1 l_3 \sin\ (\theta_i - \phi_i). \tag{6}$$

Note that prior to computing the Jacobian matrix, it is necessary to solve the inverse kinematic problem of the manipulator.

2.4. Acceleration Inversion

In RAC method, acceleration of the end-effector is used as the control signal. Therefore, the relationship between the joint and Cartesian acceleration can be extracted by differentiating Eq. (1) with respect to time.

$$J\ddot{x} + \dot{J}\dot{x} = \ddot{\theta}, \tag{7}$$

where $\ddot{x} = [\ddot{x}, \ddot{y}, \ddot{\phi}]^T$ and $\ddot{\theta} = [\ddot{\theta}_1, \ddot{\theta}_2, \ddot{\theta}_3]^T$ are the vectors of the acceleration in the Cartesian and joint spaces, respectively.

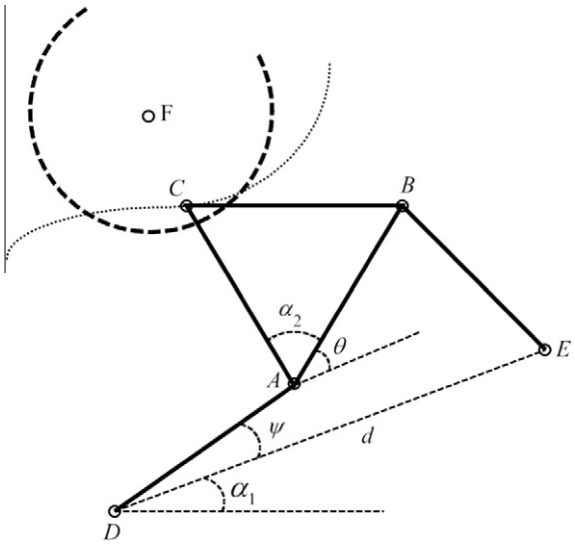

Fig. 2. Equivalent four bar linkage.

Therefore, in Eq. (7), the other quantities are assumed to be known from the velocity inversion and the only matrix that has not been defined yet is the time derivative of the Jacobian matrix denoted as $\dot{J}$. Differentiation of Eqs. (3)–(6) leads to:

$$\dot{J} = \begin{bmatrix} R_1 & S_1 & T_1 \\ R_2 & S_2 & T_2 \\ R_3 & S_3 & T_3 \end{bmatrix}, \tag{8}$$

where

$$R_i = \frac{u_i\dot{r}_i - r_i\dot{u}_i}{u_i^2}, \tag{9}$$

$$S_i = \frac{u_i\dot{s}_i - s_i\dot{u}_i}{u_i^2}, \tag{10}$$

$$T_i = \frac{u_i\dot{t}_i - t_i\dot{u}_i}{u_i^2}, \tag{11}$$

with

$$\dot{r}_i = \dot{x} + l_1\dot{\theta}_i sin\theta_i + l_2\dot{\phi}_i sin\phi_i, \tag{12}$$

$$\dot{s}_i = \dot{y} - l_1\theta_i cos\theta_i - l_2\dot{\phi}_i cos\dot{\phi}_i, \tag{13}$$

$$\dot{t}_i = l_3\dot{\phi}_i[(x - x_{oi})cos\phi_i + (y - y_{oi})sin\phi_i] + l_3[\dot{x}sin\phi_i - \dot{y}cos\phi_i] + l_1l_3(\dot{\theta}_i - \dot{\phi}_i)cos(\theta_i - \phi_i), \tag{14}$$

$$\dot{u}_i = -l_1\dot{\theta}_i[(x - x_{oi})cos\theta_i + (y - y_{oi})sin\theta_i] + l_1[\dot{x}sin\theta_i - \dot{y}cos\theta_i] + l_1l_3(\dot{\theta}_i - \dot{\phi}_i)cos(\theta_i - \phi_i), \tag{15}$$

2.5. Dynamics of 3-RRR parallel manipulator

Solving the dynamics of the system is necessary for studying the robot control strategies. To solve the dynamic models of multibody systems, first the system is considered as an equivalent tree-structure, and then by using of *d'Alembert* principle or *Lagrange* multipliers, the system constraints can be obtained [12]. Nevertheless, there are other different methods in the literature that can be used to solve the dynamics of closed kinematic chains such as virtual work [13,14], *Newton–Euler* equations [15] and *Hamilton* principle [16]. In the study, the Natural Orthogonal Complement (NOC) method is used to solve the dynamics of the 3-RRR robot. From the power equations of all the links using NOC of the constraint equations, a set of *Euler–Lagrange* equations can be derived. To control the manipulator, the direct dynamics of the system is modelled and simulated in order to predict the motion of the manipulator, given the driving forces of the system. Using NOC method introduced by Ma and Angeles, the dynamic model of the 3-RRR parallel manipulator can be expressed in the following compact form [17]:

$$M(q)\ddot{q}^a(t) + C(q,\dot{q})\dot{q}^a(t) = \tau^a, \tag{16}$$

where $q^a = [q_1, q_2, q_3]^T$ is the generalized coordinate, with q_i for $1 \leqslant i \leqslant 3$ denotes the active joint angles and $q = [q_1, q_2, \ldots, q_9]^T$ where q_i for $4 \leqslant i \leqslant 9$ represents the relative passive joint angles. $M(q) \in \Re^{3\times3}$ is the inertia matrix, $C(q\dot{q}) \in \Re^{3\times3}$ is the coefficient matrix of Coriolis and centrifugal forces and $\tau^a \in \Re^{3\times1}$ are the required torques of the actuated joints.

Direct dynamic problem is defined as obtaining the $\ddot{q}^a$, when the values of $q, \dot{q}$, and τ^a are given. In this study, direct dynamics is used to simulate the manipulator, however, in simulating process we just have τ^a, angles of active joints (q_i^a), and their respective angular velocities ($\dot{q}_i^a$). Hence, direct kinematics should be utilized to calculate q and $\dot{q}$. In direct dynamic problem Eq. (11) should be solved as a differential equation and using a suitable numerical method is necessary.

Note that further relevant kinematic and dynamic expressions applied to a 3 DOF parallel manipulator can be found in the Appendix.

3. Robot control

3.1. Resolved acceleration control

Resolved acceleration control (RAC) was first proposed by Luh et al. as an alternative method which adopts the idea of 'computed torque' technique and extends the results of 'resolved motion rate' control [18]. The RAC scheme is based on the convergence of the position error of the end-effector to zero. To guarantee the convergence of the position error of the end-effector, an input torque to the manipulator is necessary for the acceleration of the end-effector to satisfy the following expression:

$$\ddot{x}_{ref} = \ddot{x}_{des} + K_p(x_{des} - x_{act}) + K_d(\dot{x}_{des} - \dot{x}_{act}), \tag{17}$$

where $[x_{act}, \dot{x}_{act}, \ddot{x}_{act}]^T$, $[x_{des}, \dot{x}_{des}, \ddot{x}_{des}]^T$ are the vectors of the actual and desired positions, velocities and accelerations of end-effector, respectively. The position error of the end-effector can be formulated as:

$$e(t) = x_{des}(t) - x_{act}(t). \tag{18}$$

To show the influence of the input torque on the tracking error, Eq. (18) is differentiated to obtain:

$$\dot{e}(t) = \dot{x}_{des}(t) - \dot{x}_{act}(t), \tag{19}$$
$$\ddot{e}(t) = \ddot{x}_{des}(t) - \ddot{x}_{act}(t). \tag{20}$$

Then, Eq. (17) can be written as:

$$\ddot{e} + k_d\dot{e} + k_p e = 0. \tag{21}$$

Eq. (21) shows a standard form of the second-order characteristic polynomial expression. The desired performance in each component will be gradually achieved by selecting the appropriate K_p and K_d gains. A general scheme of the RAC method is shown in the Fig. 3.

For developing the FLRAC scheme, a linear RAC controller was first designed. Then, a two level FL tuning (as described in the following section) was applied to compute the PD gains of the RAC scheme in order to improve the control of the end-effector. For both approaches, the position and orientation errors of the end-effector in Cartesian space and their derivatives are defined as follows:

$$e_x = x_{des} - x_{act}, \tag{22}$$
$$\dot{e}_x = \dot{x}_{des} - \dot{x}_{act}, \tag{23}$$
$$e_y = y_{des} - y_{act}, \tag{24}$$
$$\dot{e}_y = \dot{y}_{des} - \dot{y}_{act}, \tag{25}$$
$$e_\phi = \phi_{des} - \phi_{act}, \tag{26}$$
$$\dot{e}_\phi = \dot{\phi}_{des} - \dot{\phi}_{act}. \tag{27}$$

$e = [e_x, e_y, e_\phi]$ and $\dot{e} = [\dot{e}_x, \dot{e}_y, \dot{e}_\phi]$ are position and orientation errors of the end-effector in Cartesian space and their derivatives. The parameters e and $\dot{e}$ are used as inputs to the fuzzy controller. Fig. 4 shows the proposed fuzzy resolved acceleration controller.

3.2. Two level fuzzy tuning

Since most of the recent systems are innately nonlinear and complex, fuzzy logic (FL) controller can be used as an alternative intelligent scheme to model the complex systems using a FL concept [19]. In this paper, a controller with two inputs, namely, the position and velocity errors of the end-effector, and one output with reference to the tuned parameters of the PD element in the RAC scheme was developed. The inputs and output of the fuzzy controller are normalized within range of $[-1, 1]$ and suitable scale factors have been obtained for normalization purposes based on the following conditions:

$$\hat{e} = max(-1, \min(1, S_{e_i})), \tag{28}$$
$$\hat{\dot{e}} = max(-1, \min(1, S_{ce_i})), \tag{29}$$

where $i = 1, 2, 3$ denotes the scale factors required for normalization of the position and orientation errors of the end-effector in Cartesian space. Similarly, the FL control output is normalized by using the condition, $\hat{u} = \hat{u}/\hat{u}_{max}$. Fig. 5, shows the rule-coupled fuzzy controller implemented in RAC.

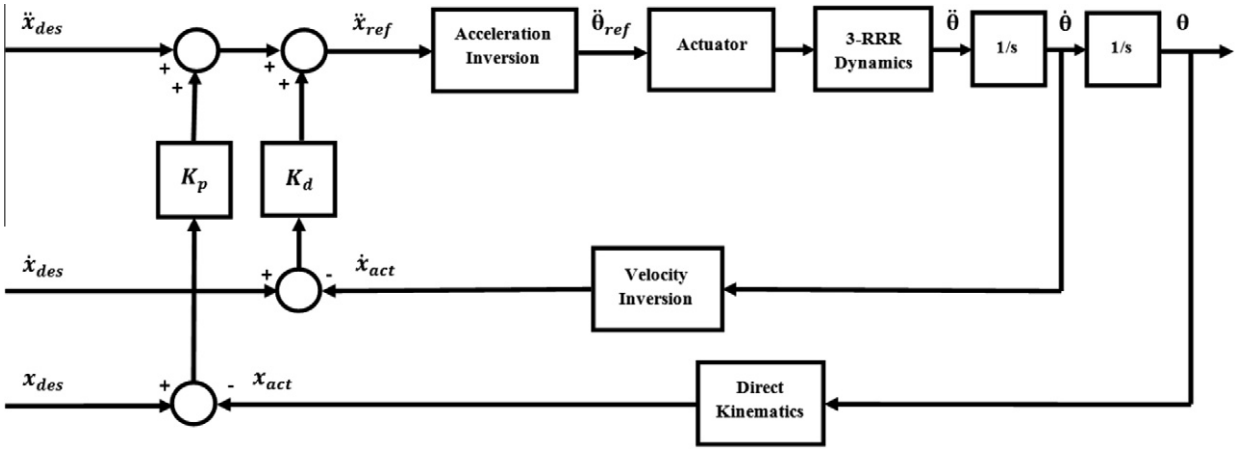

Fig. 3. Schematic diagram of the general RAC scheme.

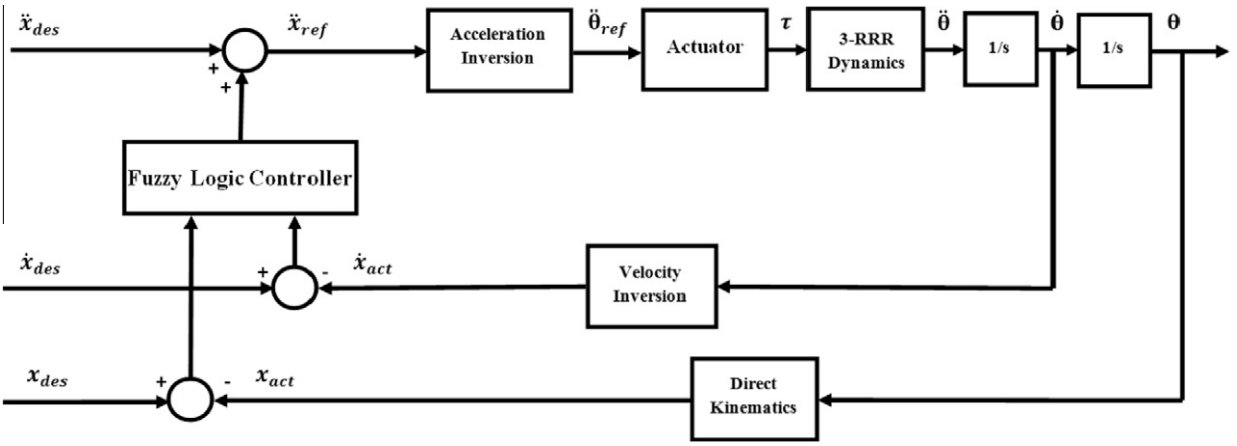

Fig. 4. Schematic diagram of the FLRAC scheme.

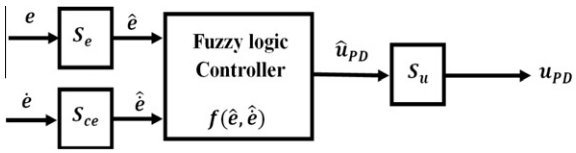

Fig. 5. Rule-coupled fuzzy PD.

For the two-input configuration used in Fig. 5, seven triangular membership functions were chosen for each input variable, and a complete rule matrix of size 7×7 is defined as:

If $\hat{e}$ is E_{wi} and $\hat{\dot{e}}$ is $\dot{E}_{wj}$ then $\hat{u}_{PD}$ is U_{i+j}

and

$$u_{PD} = S_u \hat{u}_{PD},$$

where E_{wi} and $\dot{E}_{wj}$ are input membership functions for the fuzzy controller where i is indicated as the number of inputs, and w is the number of membership functions.

Mann et al. firstly introduced a two level tuning method. For the first level which called 'linear tuning', the input and output parameters are normalized by suitable scale factors to make the fuzzy controller to act like a linear PD controller [20]. The next level of tuning is 'nonlinear tuning' in order to improve the performance of the controller without having to increase the maximum torque to the system. In nonlinear tuning level, the parameters in Fig. 6, i.e., $(S_1)_w$,$(S_2)_w$ where $w = 1,2$ of the controller should be adjusted. The appropriate values of the mentioned parameters used in the study were acquired based on those found in [20]. The membership functions representing the inputs and output of the fuzzy controller are depicted in Figs. 6 and 7.

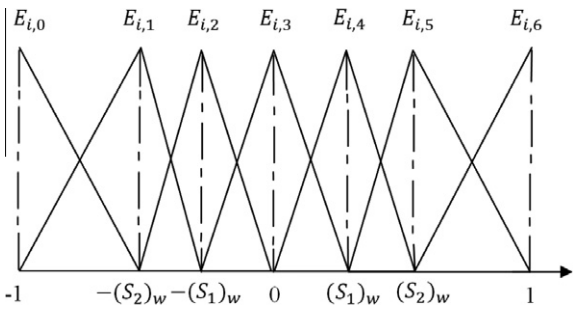

Fig. 6. Input membership function.

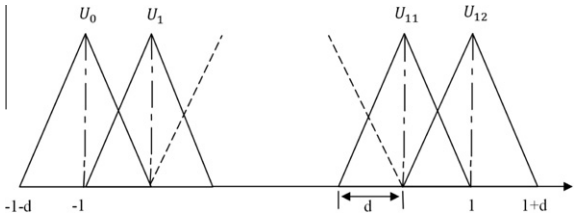

Fig. 7. Output membership function.

3.3. Active force control

During the last decade, different methods for controlling the position and force of robot manipulators have been proposed and implemented such as hybrid force/position control [21], active force control [22–24], impedance control [25] and explicit force control [26]. The main aim of these schemes is to provide a robot system to carry out the prescribed task without reducing the performance of the overall system when the loads or disturbances are applied to the robotic system. Majority of adaptive controllers which are common as robust controllers in the literature need a linearized model of the system and previous knowledge about the disturbances bounds. Furthermore, it is necessary to estimate a number of parameters or gains for the control scheme that in turn introduces more complexity to the scheme.

Active force control (AFC) method was first proposed by Hewit and Burdess in the early eighties [24]. They presented the application of the AFC technique to a robot arm in the presence of disturbances. They showed that by using this method, the system subjected to environment uncertainties, disturbances or any other changes in system parameters, remains stable and robust. The effectiveness and robustness of AFC method as a disturbance rejector scheme is proven in the literature [27]. AFC is easy to understand and very applicable because it does not need special devices to implement in real time and it only involves the computation of a number of unknown parameters necessary for the AFC loop. Therefore, it does not necessitate large computation and mathematical manipulation in order to reject the uncertainties.

From the *Newton's* second law of motion for rotational bodies, the sum of all torques applied to the system is equal to the product of the mass moment of inertia (I) and the angular acceleration (α) of the system:

$$\Sigma\tau = I\alpha. \tag{30}$$

When the disturbance is considered, Eq. (30) becomes:

$$\boldsymbol{\tau} + \boldsymbol{\tau}_d = I(\theta)\alpha, \tag{31}$$

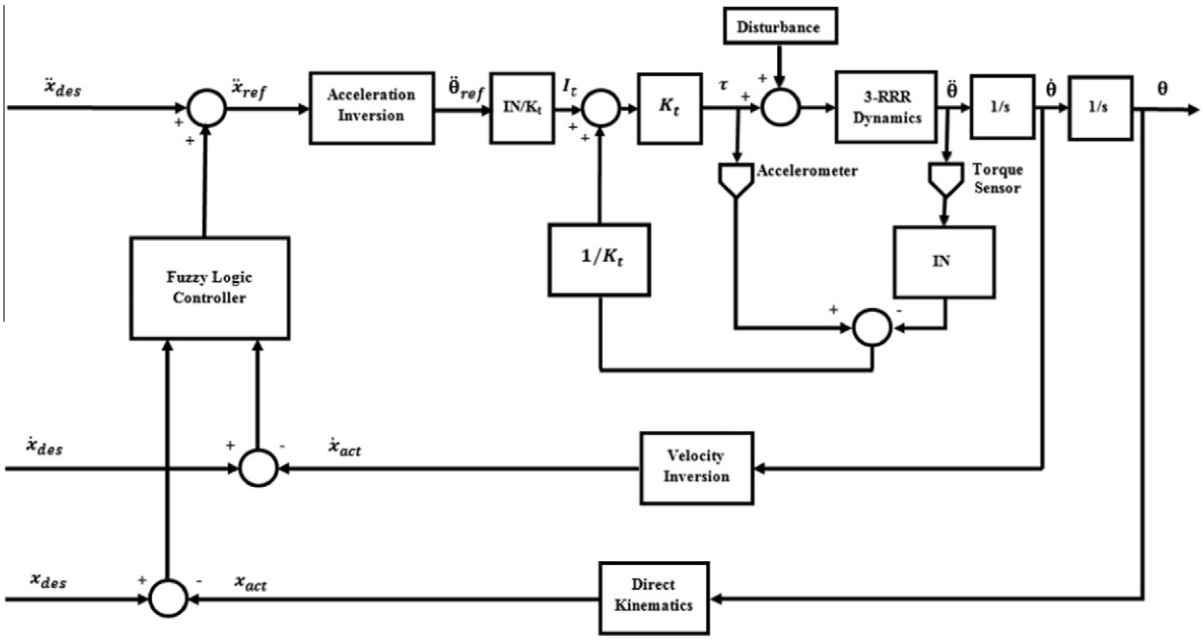

Fig. 8. Schematic diagram of the FLRAC-AFC scheme.

where,

- $\boldsymbol{\tau}$ is the applied torque to the system
- $\boldsymbol{\tau}_d$ is total applied disturbances
- θ and $\ddot{\theta}$ are the joint angle and angular acceleration of the robot system, respectively

Disturbances can be approximated as follows:

$$\boldsymbol{\tau}_d^* = \boldsymbol{\tau} - \mathbf{IN}\ddot{\theta}, \tag{32}$$

where **IN** is the estimated inertia matrix that can be obtained by crude approximation or other intelligent methods such as iterative learning, fuzzy logic and others, which crude approximation was used in this paper. $\boldsymbol{\tau}$ is the measured applied control torque that can be obtained using a torque sensor or indirectly, through a current sensor and the measured angular acceleration, i.e. $\ddot{\theta}$ using an accelerometer. From Eq. (32), it is clear that if the total applied torque to the system and angular acceleration of each actuated joint are accurately obtained and the estimated inertial matrices (**IN**) appropriately approximated, then the total disturbance torque can be computed via the AFC loop without having to acquire the exact knowledge about actual magnitude of the disturbances. A schematic diagram of the FLRAC-AFC method is depicted in Fig. 8. Note also, that, the values of **IN** were obtained via a number of trial runs based on previous research [28,29].

4. Simulation and results

To validate the effectiveness of the proposed control method, a desired end-effector's trajectory was introduced for the trajectory tracking control problem. The desired trajectory was chosen based on a butterfly shape trajectory considering the following time (t) dependent functions for the *Cartesian* coordinate:

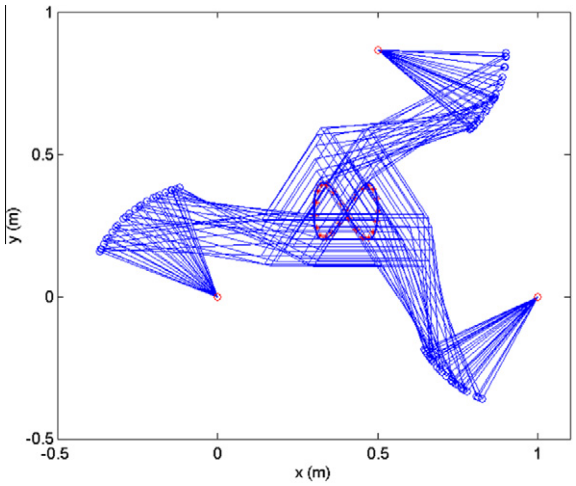

Fig. 9. Snapshots of manipulator motion.

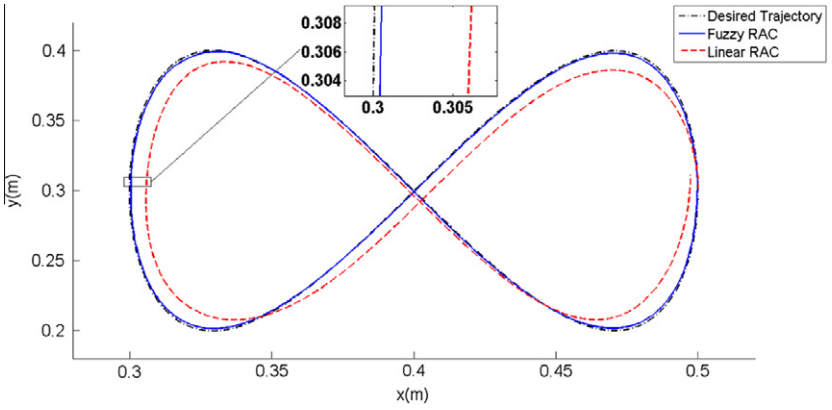

Fig. 10. Trajectory tracking of the end-effector using linear RAC and FLRAC in absence of disturbances.

$$x_p = x_{p0} + 0.1\cos(0.4 \times \pi \times t) \quad 0 \leqslant t \lll 5s, \tag{33}$$

$$y_p = y_{p0} + 0.1\sin(0.8 \times \pi \times t) \quad 0 \leqslant t \lll 5s. \tag{34}$$

To simulate the dynamics and control of the 3-RRR parallel robot, MATLAB/Simulink software was used. The geometric dimensions and other properties of the manipulator and the controllers' parameters are as follows:

$$l_1 = 0.4\ \text{m}, \quad l_2 = 0.6\ \text{m}, \quad l_3' = 0.4\ \text{m}$$

$$m_1 = m_2 = m_3 = 3\ \text{kg}, \quad I_1 = I_2 = I_3 = 0.04\ \text{kg m}^2$$

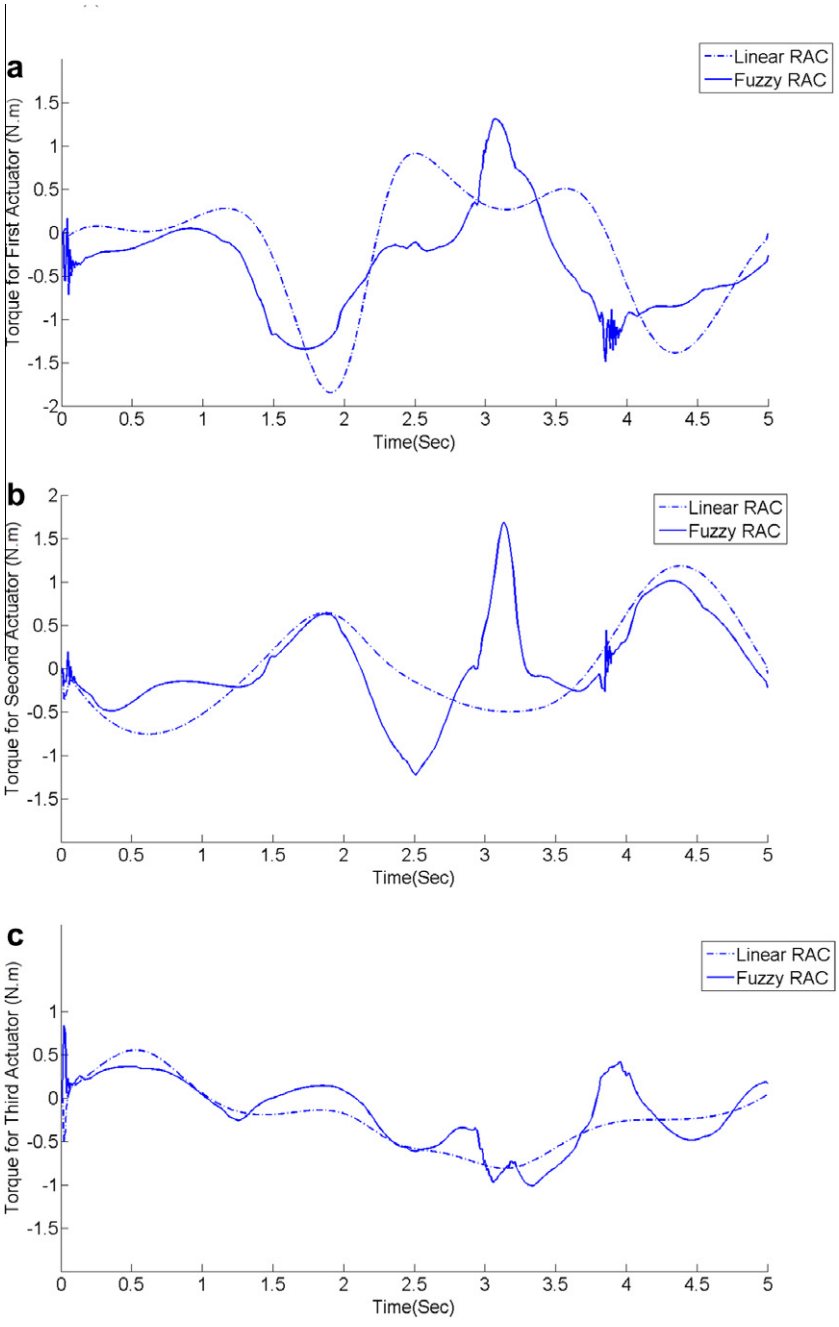

Fig. 11. (a)–(c) Required torques for three actuated joints using linear RAC and FLRAC.

$m_4 = m_5 = m_6 = 1$ kg, $I_4 = I_5 = I_6 = 0.12$ kg m^2

$m_7 = 8$ kg, $I_7 = 0.0817$ kg m^2

RAC : $K_p = 60$, $K_i = 0$, $K_d = 40$

Inertia for the AFC loop $\mathbf{IN} = [0.1\ 0.1\ 0.1]$ kg m^2

Harmonic disturbance to the first actuated joint: $\tau_h = 20 \sin 50t$ Nm

Fig. 9 shows snapshots of a series of the manipulator's movements in tracking the desired trajectory. From the figure, it can be seen that the desired trajectory is within the manipulator's workspace. Also, there is no singularity observed while the manipulator is describing the prescribed trajectory. The whole process took approximately 5 seconds.

As mentioned earlier, first, a linear RAC scheme was implemented to the manipulator to control the Cartesian trajectory tracking of the end-effector. The PD gains of RAC outer-loop were heuristically tuned after a number of trial runs, taking into account the initial ideal situation, i.e. in the absence of disturbances. Then, the required parameters of the fuzzy controllers such as normalizing scale factors and optimum linear PD gains of the RAC were obtained and substituted in Eq. (17). Results for the linear RAC and FLRAC are depicted in Fig. 10, which demonstrates the better performance of the FLRAC compared to linear RAC.

Fig. 11(a)–(c) show the applied torques to each actuated joint by the two controllers. From the figures, it can be seen that the maximum required torque for each actuated joint to produce the desired trajectory are nearly the same, implying that powers or energies required to drive the three links via the joints are comparable. There are some small fluctuations observed in the fuzzy RAC scheme as depicted in Fig. 11(a) and (b) which are probably due to the fuzzy estimation and adaptation process when the manipulator operates to perform the trajectory tracking task. The magnitude and period of the oscillation are however very small and transitory. This has no profound effect on the actual tracking performance of the manipulator as the result in Fig. 10 portrays.

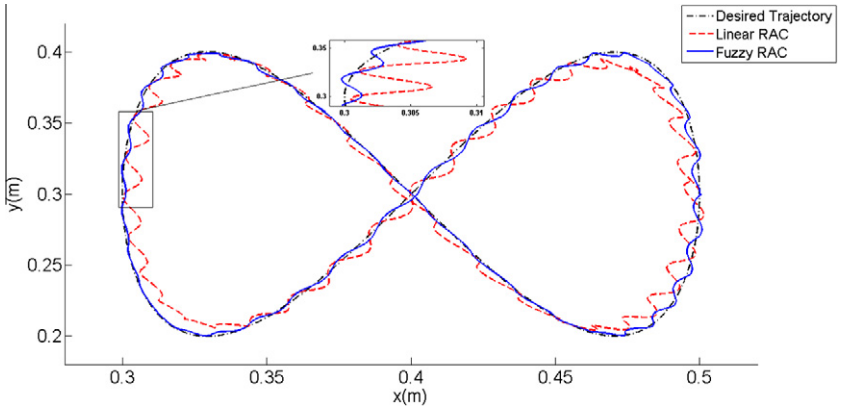

Fig. 12. Trajectory tracking of the end-effector using linear RAC and FLRAC in presence of disturbances.

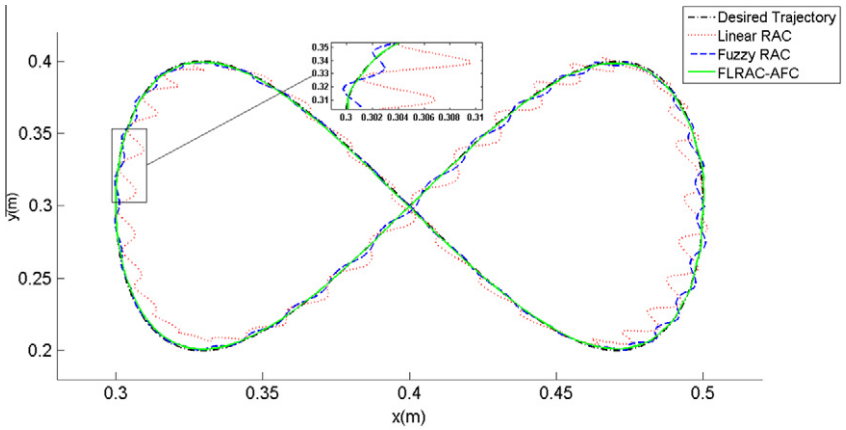

Fig. 13. Trajectory tracking of the end-effector using linear RAC, FLRAC, and FLRAC-AFC in presence of disturbances.

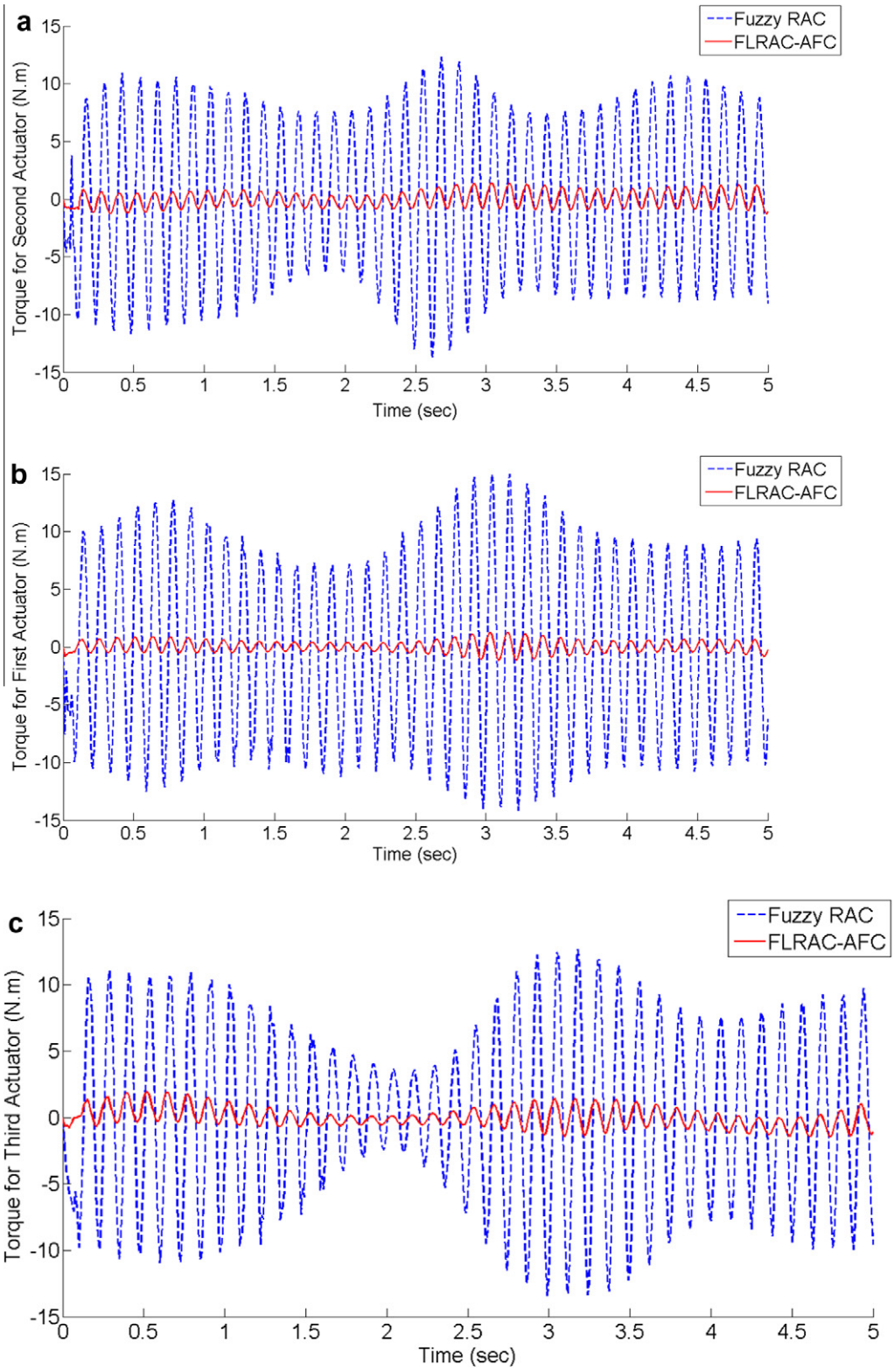

Fig. 14. (a)–(c) Required torques for three actuated joints using FLRAC and FLRAC-AFC.

Later, a known harmonic disturbance was introduced into the first actuated joint. The results obtained for both the linear RAC and FLRAC controller were presented and compared. From Fig. 12, it is clear that the system performance is significantly

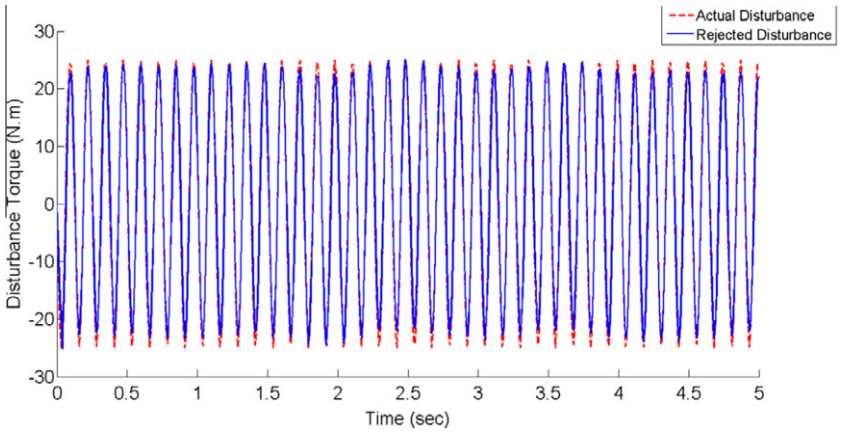

Fig. 15. Applied disturbances versus rejected disturbances using FLRAC-AFC.

distorted in both linear RAC and FLRAC schemes. However, the latter produces a comparatively better response from the desired trajectory than the former.

In order to eliminate the trajectory distortion caused by the disturbance, a second degree of freedom controller namely active force control (AFC) loop was added in cascade form with the FLRAC scheme. The results in Fig. 13, clearly illustrate the robustness and effectiveness of the proposed FLRAC-AFC scheme to improve the overall system dynamic performance particularly when the manipulator is subjected to the disturbances compared to the FLRAC and linear RAC alone.

In Fig. 14(a)–(c), the required torques of actuated joints for the manipulator to follow the prescribed trajectory are illustrated and compared for FLRAC and FLRAC-AFC schemes. From the figures, it can be concluded that, the torques applied to each actuator by FLRAC scheme in order to reject the disturbances are relatively higher in magnitude than in FLRAC-AFC scheme. This may eventually cause saturation in the actuators. On the other hand, FLRAC-AFC scheme is able to reject the disturbances effectively without having to increase the torques of the actuated joints.

Fig. 15 shows the actual disturbance applied to the system and the rejected disturbance that is estimated by using the FLRAC-AFC scheme over time.

5. Conclusion

A novel 2-DOF control scheme comprising a two level fuzzy tuning resolved acceleration control with active force control (FLRAC-AFC) was developed and implemented to the 3-RRR manipulator to provide an excellent coordinated trajectory tracking performance of the system in the presence of the introduced disturbances. Both the first and second level of fuzzy tunings are found to be very effective in computing the desired parameters of the FLRAC component even while the manipulator is executing its trajectory tracking task. Results clearly show that the linear RAC method, though simple and relatively stable, could not provide satisfactory performance in the presence of introduced harmonic disturbance as system shows a high degree of inaccuracy as can be seen through the greatly distorted tracked trajectory. This is in stark contrast with the proposed intelligent AFC-based method, i.e., FLRAC-AFC in which the manipulator exhibits excellent and robust tracking capability. The scheme is able to reject the disturbances without having to increase the magnitudes of the actuated torques at the joints. Further works could include the possibility of performing comprehensive sensitivity analysis based on other loading and operating environments to include parametric changes and uncertainties.

Appendix A

A.1. Inverse kinematic solution

A general solution of the inverse kinematic for leg i is expressed as follows [11]:

$$\theta_i = \alpha_i \pm \psi, \quad i = 1,2,3, \tag{A.1}$$

$$\alpha_i = \text{atan2}(x_{2i}, y_{2i}). \tag{A.2}$$

ψ_i can be obtained as follows:

$$\psi_i = \cos^{-1}\left[\frac{l_i^2 - l_2^2 + x_{2i}^2 + y_{yi}^2}{2l_i\sqrt{x_{2i}^2 + y_{2i}^2}}\right], \quad 0 \leqslant \psi \leqslant \pi. \tag{A.3}$$

Coordinates x_{2i} and y_{2i} are defined as:

$$x_{2i} = x - l_3 \cos\phi_i - x_{oi}, \tag{A.4}$$

$$y_{2i} = y - l_3 \sin\phi_i - y_{oi}, \tag{A.5}$$

where angles $\{\phi_i\}_1^3$ are given by:

$$\phi_1 = \phi + \frac{\pi}{6}, \tag{A.6}$$

$$\phi_2 = \phi + \frac{5\pi}{6}, \tag{A.7}$$

$$\phi_3 = \phi - \frac{\pi}{2}. \tag{A.8}$$

The Cartesian positions of centers of the motors are considered as follows:

$$x_{oi} = \left\{0, 1, \frac{1}{2}\right\}, \tag{A.9}$$

$$y_{oi} = \left\{0, 0, \frac{\sqrt{3}}{2}\right\}. \tag{A.10}$$

A.2. Direct kinematic solution

Point C in Fig. 2 is a point of the coupler link generating a coupler curve. A solution for the closure of the whole kinematic chain is determined via the contraction of the circle and the coupler curve with the following set of equations will be obtained [11]:

$$x_{23} = x_{11} + l_2 \cos(\alpha_1 + \psi) + \sqrt{3} l_3 \cos(\alpha_1 + \alpha_2 + \theta), \tag{A.11}$$

$$y_{23} = x_{11} + l_2 \sin(\alpha_1 + \psi) + \sqrt{3} l_3 \sin(\alpha_1 + \alpha_2 + \theta) \tag{A.12}$$

and

$$\alpha_1 = \text{atan2}\left[\frac{y_{12} - y_{11}}{x_{12} - x_{11}}\right], \quad \alpha_2 = \frac{\pi}{3}, \tag{A.13}$$

$$\theta(1), \theta(2) = 2\tan^{-1}\left[\frac{b \pm \sqrt{b^2 - ac}}{a}\right]. \tag{A.14}$$

a, b, c are given as follows:

$$a = \frac{-d^2 - 3l_3^2}{2\sqrt{3} l_2 l_3} - \frac{d}{l_2} + \left(1 + \frac{d}{\sqrt{3} l_3}\right) \cos\psi, \tag{A.15}$$

$$b = \sin\psi, \tag{A.16}$$

$$c = \frac{-d^2 - 3l_3^2}{2\sqrt{3} l_2 l_3} + \frac{d}{l_2} + \left(\frac{d}{\sqrt{3} l_3} - 1\right) \cos\psi, \tag{A.17}$$

where

$$d = \sqrt{(x_E - x_D)^2 + (y_E - y_D)^2}. \tag{A.18}$$

The coupler curve intersects the circle defined by the rotation of link FC around point F. Therefore, the nonlinear equation to be solved is given by:

$$(x_C - x_F)^2 + (y_C - y_F)^2 = l_2^2 \tag{A.19}$$

Eq. (A.19) can be solved for angle ψ using a numerical procedure. Direct kinematics of manipulator is vital for the system control objectives.

A.3. Dynamic solution

The general form of the dynamics solution can be written as follows [17]:

$$\mathbf{N}^T \mathbf{M}_{total} \mathbf{N} \ddot{q} + (\mathbf{N}^T \mathbf{M}_{\mathbf{total}} \dot{\mathbf{N}} + \mathbf{N}^T \boldsymbol{\Omega} \mathbf{M}_{\mathbf{total}} \mathbf{N}) \dot{\mathbf{q}}^a - \mathbf{N}^T \mathbf{W}^g = \boldsymbol{\tau}^a, \tag{A.20}$$

where **N** is the NOC matrix, **M** and **Ω** are diagonal matrices defined as:

$$\mathbf{M_{total}} = \mathrm{diag}(\mathbf{M}_1, \mathbf{M}_2, \ldots \mathbf{M}_r), \tag{A.21}$$

$$\boldsymbol{\Omega} = \mathrm{diag}(\boldsymbol{\Omega}_1, \boldsymbol{\Omega}_2, \ldots \boldsymbol{\Omega}_T) \tag{A.22}$$

and

$$\mathbf{W}^g = \begin{bmatrix} \mathbf{0} \\ m_1\mathbf{g} \\ 0 \\ m_2\mathbf{g} \\ \cdot \\ \cdot \\ \cdot \\ \mathbf{0} \\ m_r\mathbf{g} \end{bmatrix}. \tag{A.23}$$

The zeroes (**0**) in Eq. (A.23) represent the 3-D zero vector and **g** is the gravity acceleration vector, respectively. m_r are the masses of the movable rigid bodies. Note also, that, $r = 1,2,\ldots,7$ denote the number of movable rigid bodies in the system. Eq. (A.20) can be simplified by considering the following expressions:

$$\mathbf{M} = \mathbf{M}(q) = \mathbf{N}^T\mathbf{M}_{total}\mathbf{N}, \tag{A.24}$$

$$\mathbf{C} = \mathbf{C}(q, \dot{q}) = \mathbf{N}^T\mathbf{M}_{total}\dot{\mathbf{N}} + \mathbf{N}^T\boldsymbol{\Omega}\mathbf{M}_{total}\mathbf{N}, \tag{A.25}$$

$$\mathbf{G} = \mathbf{G}(q) = -\mathbf{N}^T\mathbf{W}^g. \tag{A.26}$$

Therefore the equation becomes:

$$\mathbf{M}\ddot{q} + \mathbf{C}\dot{q}^a + \mathbf{G} = \boldsymbol{\tau}^a, \tag{A.42}$$

where $q^q, \dot{q}^a$ and $\ddot{q}^a$ are the corresponding displacement, velocity and acceleration of the actuated joints, respectively.

References

[1] J.P. Merlet, Parallel Robots, Kluwer Academic Publishers., 2000.
[2] V.E. Gough, Contribution to discussion of papers on research in automotive stability, control and tyre performance, Proc. Auto Div. Inst. Mech. Eng. 171 (1956) 392–395.
[3] D. Stewart, A platform with 6 degree of freedom, Proc. Auto Div. Inst. Mech. Eng. 180 (15) (1965) 371–386.
[4] K.M. Lee, C. Yien, Design and control of a prototype platform manipulator for work handling applications, J. Mech. Work. Technol. 20 (1989) 305–314.
[5] F. Behi, M. Mehregany, K. Gabriel, A microfabricated three degree of freedom parallel mechanism, Proc. IEEE Microelectron. Mech. Syst. (1990) 159–165.
[6] F. Ghorbel, O. Chetelat, R. Longchamp, On the modeling and control of closed-chain mechanisms, Proc. IMACS/IEEE Int. Conf. Comput. Eng. Syst. Appl. (1998) 714–720.
[7] M.W. Walker, Adaptive control of manipulators containing closed kinematic loops, IEEE Trans. Robot. Autom. 6 (1) (1990) 10–19.
[8] M. Honegger, A. Codourey, E. Burdet, Adaptive control of the hexaglide, a 6 DOF parallel manipulator, Proc. IEEE Int. Conf. Robot. Autom. (1997) 543–548.
[9] B.K. Yoo, W.C. Ham, Adaptive control of robot manipulator using fuzzy compensator, IEEE Trans. Fuzzy Syst. (8) (2000) 186–199.
[10] S.D. Stan, G. Gogu, M. Manic, R. Balan, C. Rad, Fuzzy control of a three degree of freedom parallel robot, Technol. Dev. Educ. Autom. (2010) 437–442.
[11] C. Gosselin, J. Angeles, Kinematics of Parallel Manipulators, PhD Thesis, McGill University Montreal, Quebec, Canada, 1989.
[12] M.J. Liu, C.X. Li, C.N. Li, Dynamics analysis of the Gough–Stewart platform manipulator, IEEE Trans. Robot. Autom. 16 (1) (2000) 94–98.
[13] J. Gallardo, J.M. Rico, A. Frisoli, Dynamics of parallel manipulators by means of screw theory, Mech. Mach. Theory. 38 (11) (2003) 1113–1131.
[14] L.W. Tsai, Solving the inverse dynamics of a Stewart-Gough manipulator by the principle of virtual work, ASME. J. Mech. Des. 122 (1) (2000) 3–9.
[15] B. Dasgupta, P. Choudhury, A general strategy based on the Newton–Euler approach for the dynamic formulation of parallel manipulators, Mech. Mach. Theory 34 (6) (1999) 801–824.
[16] K. Miller, Optimal design and modeling of spatial parallel manipulators, Int. J. Robot. Res. 23 (2) (2004) 127–140.
[17] O. Ma, J. Angeles, Direct kinematics and dynamics of a planar 3-DOF parallel manipulator, Proc. ASME Conf. Des. Autom. 3 (1989) 313–320.
[18] J.Y.S. Luh, M.W. Walker, R.P. Paul, Resolved acceleration control of mechanical manipulators, IEEE Trans. Autom. Control 25 (3) (1980) 468–474.
[19] A.L. Zadeh, Fuzzy sets, Inf. Control 8 (1965) 338–353.
[20] G.K.I. Mann, B.G. Hu, R.G. Gosine, Two-Level Tuning of Fuzzy PID Controllers, IEEE Trans. Syst. Man. Cybern 31 (2) (2001).
[21] M.H. Raibert, J.J. Craig, Hybrid position/force control of manipulators, J. Dyn. Syst. Meas. Control 102 (1981) 126–133.
[22] M. Nakao, K. Ohnishi, K. Miyachi, A robust decentralized joint control based on interference estimation, Proc. IEEE Int. Conf. Robot. Autom. 1 (1987) 326–331.
[23] M. Shibata, T. Murakami, K. Ohnishi, A unified approach to position and force control by fuzzy logic, IEEE Trans. Ind. Electron. 43 (1) (1996) 81–87.
[24] J.R. Hewit, J.S. Burdess, Fast dynamic decoupled control for robotics using active force control, Mech. Mach. Theory. 16 (5) (1981) 535–542.
[25] H. Kazerooni, T.B. Sheridan, P.K. Houpt, Robust compliant motion for manipulators. Part 1: The fundamental concepts of compliant motion; Part 2: Design method, IEEE J. Robot. Autom. (1986) 83–105.
[26] R. Volpe, P. Khosla, A theoretical and experimental investigation of the explicit force control strategies for manipulators, IEEE Trans. Autom. Control 38 (11) (1993) 1634–1650.
[27] M. Mailah, Intelligent Active Force Control of a Rigid Robot Arm Using Neural Network and Iterative Learning Algorithms, PhD Thesis, Univ. of Dundee, UK, 1998.
[28] A. Noshadi, M. Mailah, A. Zolfagharian, Active force control of 3-RRR planar parallel manipulator, IEEE Int. Conf. Mech. Electron. Tech. (2010) 77–81.
[29] A. Noshadi, A. Zolfagharian, M. Mailah, Performance analysis of the computed torque based active force control for a planar parallel manipulator, IEEE Int. Conf. Mech. Aerosp. Eng. (2010) 142–148.